

Process parameters and properties of electric resistance spot welded AISI304-AISI1020 dissimilar weldments

Mathi Kannaiyan^a, Jinu GowthamiThankachi Raghuvaran^{b*}, Karthikeyan Govindan^c and Elaya Perumal Annamalai^d

^aAssistant Professor, Department of Mechanical Engineering, University College of Engineering, Kancheepuram, Tamil Nadu

^bAssistant Professor, Department of Mechanical Engineering, University College of Engineering, Nagercoil, Konam, Tamil Nadu

^cAssistant Professor, Department of Mechanical Engineering, University College of Engineering, Pattukkottai, Rajamadam Tamil Nadu

^dResearch Scholar/SRF (UGC), Department of Mechanical Engineering, University College of Engineering, Nagercoil, Konam, Tamil Nadu

In this present work, an attempt was made on optimising the Resistance Spot Welding (RSW) process parameters for joining two dissimilar combinations of AISI 304 and AISI 1020 grade steel with each other. Experiments were conducted by varying the three weld process parameters such as welding current, pressure and welding time. The integrity of the weld joints was evaluated mechanically and metallurgically. Tensile shear fracture, nugget diameter, and hardness properties were examined. Macrostructure, Microstructure, and Scanning Electron Microscopy (SEM) analysis were carried out on the tested samples to validate the type of fracture occurred. Maximum nugget diameter and maximum tensile fracture of 6.666 mm and 10.5 kN were achieved respectively. The experimental results confirmed the validity of the used Response Surface Methodology applied for optimising the welding process parameter in the RSW process. The Response Surface Methodology (RSM) results show that the weld current is the most significant factor for Tensile Shear Fracture Load (TSFL) and nugget diameter, followed by weld pressure and time.

Keywords: Resistance spot welding, Tensile shear fracture, Nugget diameter, Response surface methodology.

Introduction

The RSW process is widely used for joining sheet metals in automobile sectors due to the increase in the demand for welding. In automobiles industries fabrication of sheet metals are ideally suited for mass production due to inexpensive and effective way to join metal sheets [1, 2]. In RSW process the two sheet metals are joined in the form of a spot or continuous faying method. The process of joining the sheet can be completed in three stages namely squeeze time, weld time/heating time and hold time. In this welding process a substantial electric current is allowed to flow on the sheets which are placed together, and pressure is applied with the help of two copper electrode tips. Due to the flow of welding current against the sheets, the resistive path is generated at the area to be joined, which creates localized heating. When the flow of current is stopped, it gets solidify to join the sheets. The efficiency of the joints was based on the weld process parameters such as welding current, welding time as well as electrode pressure between the two water-cooled copper-based

electrodes [3]. Vuril *et al.* investigated the effect of nugget diameter on mechanical and metallurgical properties of galvanised steel and AISI304 welded lap joints [4]. Bouyousfi *et al.* [5] carried out experiments to investigate the effect of spot welding process on mechanical characteristics of AISI 304 similar joints. They revealed that the applied load is a major controlling factor for the mechanical characteristics of weld joint compared to the welding duration and current intensity of welding. Oscar Martin *et al.* [6] carried out spot welding on austenitic stainless steel(304), and the results revealed that the tensile shear load bearing capacity (TSLBC) increased initially by increasing weld time and weld current, but when the pressure increases continuously the TSLBC was decreased. Yoon *et al.* [7] identified the optimal weld process parameters for spot welding of AA7075- T6 aluminium alloy sheets using Taguchi method. They found that Electrode force 1323 N, Welding current 14 kA, Welding time four cycles is the optimum process parameter for obtaining higher tensile shear strength.

Austenitic stainless steel and low carbon steel possess an excellent combination of mechanical properties, formability, weldability and corrosion resistance. This combination of steels is extensively used in the marine industry [8, 9]. Stainless steel is an iron-based alloy

*Corresponding author:
Tel : +919443994330
Fax: 04652-260510
E-mail: grjnu1980@gmail.com

having excellent corrosion resistance due to the passive films on the surface [10, 11]. This type of materials is used in several applications due to its superior properties such as high corrosion resistance, good toughness, high energy absorption, weldability, and high strength [12]. Stainless steel has been widely used in automotive and aerospace industries due to its higher corrosion resistance and workability [13, 14]. Jae Hyung Kima investigated the impact of weld input process parameters like weld time and current of resistance spot welding with output responses like tensile strength and nugget diameter on Low Carbon and High strength Low Alloy (HSLA) Steel [15]. Dawei Zhao [16] investigated the effect of the specific transition resistance on sheet-sheet contact. They revealed that the sheet to sheet contact possesses ten times higher specific transition resistance than between electrodes to sheet contact. They also concluded that the local contact temperature is the most significant influencing factor for the specific transition resistance. Aslanlar *et al.* [17] analysed the effect of variation in dynamic resistance across electrodes for the nugget growth by varying the RSW parameters such as electrode force and welding current. They identified that for higher weld, current and electrode force improves the rate of nugget growth.

From the literature survey, it is identified that several researchers have shown a keen interest in resistance spot welding process for welding of various similar and dissimilar joints using duplex stainless steel, HSLA steels, AA 7075. The various mechanical and metallurgical investigations were also carried out on the resistance spot-welded joints based on its applications. No work was carried out for identifying the optimum RSW process parameters in welding of AISI 304 and AISI 1020 dissimilar joints.

Therefore in this work, Electrical Resistance spot welding of single lap joint was carried out on AISI 304 and AISI 1020 materials by varying the weld process parameters such as welding power, welding pressure and weld time. The various mechanical tests, such as tensile shear fracture and hardness, were conducted on the welded samples to find the relationship between weld input process parameters and the resulting weld nugget strength. In this work RSM was used to predict the tensile shear strength/failure modes of welded joint at various RSW process parameters.

Experimental Procedure

In this work AISI 304 with chromium as an alloying element and AISI 1020 with manganese as an alloying element of 1.5 mm as thickness were used in this present investigation as shown in Fig. 1(a) and (b). The mechanical, thermal properties and chemical composition of these alloys are given in Table 1 and 2.

The joining of metal sheets was carried out in Resistance spot welding machine with the configuration of pedestal

type inverter base and medium frequency DC machine (Model PACI TECH-ERSW) of capacity 90 kV. It has the flexibility of welding sheets up to 6 mm thickness with a maximum current of 20 kVA capacities shown in Fig. 1(c). The electrode used in this welding consists of a shank of diameter 16 mm with a conical cap having a tip diameter of 5 mm shown in Fig. 1(d), which is made up of Cu-Cr-Zr alloy and is water-cooled during the welding process. The electrodes are made to hold the sheet specimens under pre-determined pressure, and at that time the current is passed through it, to fabricate the joints. Three process parameters with three levels of experiments were selected as given in Table 3. The welded samples are shown in Fig. 1(e). The tensile shear test was conducted on the welded samples as per the ISO14273 standards. The width of the samples is calculated as 41.285 mm, and it was rounded to 42 mm by using the equation

$$w \geq wcr = 13:4 + 18:59 t \quad (1)$$

The nugget diameter was measured by a digital calliper. Investigating the weld nugget resistance was carried out with the help of computerised Micro Vickers hardness tester under the application of load 200 gms for 15 seconds of dwell period. The optical system, which is used for measuring of nugget zone, has a range of 200 μ m at 0.01 μ m of resolution by a light source of 12 V/20 W ARTRAY Camera.

For microstructural analysis, the welded samples were polished by different grit papers and etched to reveal microstructure. A Carl Zeiss Ultra Plus Gemini FESEM model SEM was used to characterise the weld zones of the welded samples.

Result and Discussions

Heat input is one of the main criteria for obtaining the efficiency of the joint. Also, the capability is based upon the differences in the melting temperature of the two dissimilar metals. The adequate heat generation depends on the variation of the three parameters. (1) The current, (2) the resistance of the conductor and (3) the duration of the current. The required heat generated through the electrical resistance of the two bodies to be joined specified in Eq. (1) [18, 19].

$$Q = I^2 R t \quad (2)$$

where t = Time to current flow in -s

I = Current in- A

R = Electrical resistance in- ohm

Q = Heat generated in- J

According to Joule's law as welding current decreases with increasing electrical resistance and induction of constant second voltage. When heat input is increased

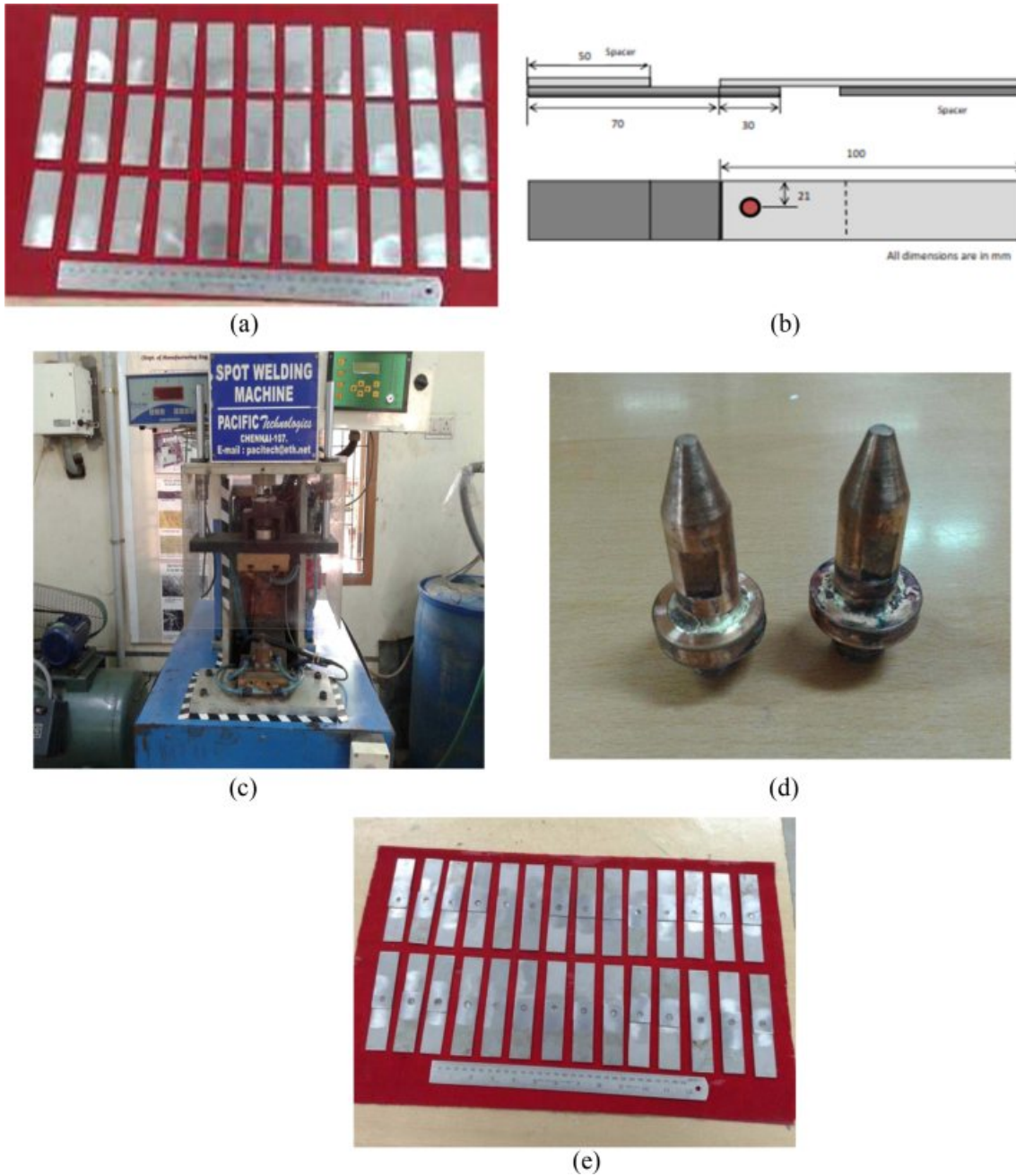


Fig. 1. (a) base metal specimen, (b) specification of base metal, (c) resistance spot welding machine, (d) copper electrode, and (e) welded specimen.

Table 1. Mechanical and thermal properties of base metal.

Materials	Density (kg/m ³)	Young's modulus (GPa)	Coefficient of thermal expansion (µm/m/°C)	Thermal conductivity (W/m k)	Specific heat (J/kg/K)	Electrical resistivity (Ωm)
AISI 304	8030	193	17.8	21.5	500	7.2 10 ⁻⁷
AISI1020	7800	206	10.98	39.77	452	6.48 10 ⁻⁷

Table 2. Chemical composition of base materials.

Alloy	Cr (%)	Ni (%)	C (%)	S (%)	Si (%)	Mn (%)	Mg (%)	P (%)	Fe
AISI304	18.2	8.21	0.064	0.002	0.28	1.01	-	0.079	Remaining
AISI1020	0.08	0.04	0.2	0.049	0.26	0.56	0.1	0.019	Remaining

weld nugget also increased similar reports were identified in [19-22].

Design of experiments

Based on previous literature's and by conducting feasibility weld trials, it is identified that the most influencing process parameter for RSW process is power, pressure and weld time. Similarly, from the feasibility study the range of parameters were identified to obtain defect-free joints. The selected weld process parameters and their levels are listed in Table 3, by applying those values in Box-Behnken (three-parameter and three levels).

The 17 combinations of weld process parameters were collected as given in Table 4; the weld trials were conducted. From the welded samples the TSFL and hardness test was carried out, and the results are given in Table 4. The nugget diameter and depth was also measured and given in Table 4.

From the Table 4, it is identified that the maximum TSFL of 10.5 kN and hardness 543 VHN was obtained for the joint welded at the power of 65 watts, the pressure of 3.8 kN and the weld time of 2 seconds. The main parameter in this research is the nugget diameters which decide the joint efficiency, and it is measured by a video measuring instrument, and the results are

tabulated in Table 4. The maximum efficiency of the joint depends on increasing the weld time and current. The nugget diameter is varied from 4.612 mm to 6.666 mm. This varied nugget diameter will affect the change in tensile shear fracture [23].

In resistance spot welding, the pressure and current applied on the lap joined metals and which will attain molten metal and solidified into nugget after quick cooling. The low, medium, high TSFL values obtained samples are subjected to macro-structural evaluation, and the corresponding macro images are given in Table 5. Vural and Akku [4] also reported that the heat input increases with increasing weld time and current the varied macrostructure which are shown in the figures and presented in Table 5. reveal that the shearing and tearing occurred on the welded joints.

Analysis Of Variance (ANOVA)

In order to identify the influence of weld process parameters on the quality of weld joints. It is necessary to find out the optimal condition of process parameter levels, which were done with the help of ANOVA. ANOVA was performed based on the experimental data at a confidence interval of 95%. The obtained results from the ANOVA analysis are given in Table 6. From Table 6, it is identified that the model P-value of 11.96 implies that the model is an important one. Similarly, the R- squared value of 0.9389 and the adjacent R squared value of- 0.8304 reveal the same results. From Table 6, it is identified that the weld current is the most significant factor for TSFL and nugget diameter, followed by the weld pressure. Weld time is the least significant factor for the above output parameters.

Table 3. Process Parameters and their levels.

Parameters	Unit	Symbol	Levels		
			Low (-1)	Medium (0)	High (+1)
POWER	(W)	A	55	60	65
PRESSURE	(kN)	B	3.4	3.6	3.8
TIME	(s)	C	1.5	2	2.5

Table 4. Input/output values for coded values.

S.No	Power (A) (W)	Pressure (B) kN	Time (C) (sec)	TSFL (R1) (kN)	Hardness (VHN)	Nugget Diameter (mm)	Nugget Depth (mm)
1	1	1	0	10.5	543	6.666	0.06±0.01
2	0	1	1	8.9	473	5.431	0.09±0.01
3	0	0	0	8.7	455	5.297	0.06±0.01
4	0	-1	1	7.9	423	5.012	0.12±0.01
5	1	-1	0	9.3	471	5.652	0.11±0.01
6	0	1	-1	7.2	412	4.949	0.09±0.01
7	0	1	0	9.8	519	6.213	0.42±0.01
8	-1	0	-1	6.1	359	4.813	0.40±0.01
9	0	-1	-1	8.1	426	5.015	0.14±0.01
10	-1	0	1	6	369	4.612	0.25±0.01
11	1	0	-1	9.5	502	5.897	0.28±0.01
12	0	0	0	8.8	455	5.297	0.48±0.01
13	0	0	0	9.1	482	6.42	0.34±0.01
14	0	0	0	9.5	498	6.39	0.39±0.01
15	1	0	1	9.5	509	5.897	0.33±0.01
16	-1	-1	0	7.1	409	4.876	0.026±0.0
17	-1	1	0	7.3	428	4.978	0.0249±0.01

Table 5 Macrostructure evaluations for Resistance spot welded Joints at high, medium and low levels.

TSFL (kN)	Cross-Sectional macro structure	Nugget (mm)	Top view of top sheet	Bottom view of top sheet	Top view of bottom sheet
High (10.5)					
Medium (9.5)					
Low (6.1)					

Table 6. ANOVA for response surface quadratic model analysis of variance of partial sum of squares type III.

Source	Sum of squares	Degrees of freedom	Mean squares	F - Value	p-Value	Prob >F
Model Significant		25.83	9	2.87	11.96	0.0018
A-A	18.91	1	18.91	78.77	<0.0001	
B-B	0.28	11	0.28	1.17	0.315	
C-C	0.24	1	0.24	1.02	0.346	
AB	0.25	1	0.25	1.04	0.3415	
AC	2.500E-0.03	1	2.500E-0.03	0.01	0.9216	
BC	0.9	1	0.9	3.76	0.937	
A2	0.82	1	0.82	3.4	0.1079	
B2	0.15	1	0.15	0.63	0.4523	
C2	3.92	1	3.92	16.33	0.0049	
Residual		1.68	7	0.24		
Lack of Fit		0.81	3	0.27	1.25	0.4034 Not significant
Pure Error		0.87	4	0.22		
Cor. Total		27.52	16			

The Model P-value of 11.96 implies the model is significant. And also there is only R-Squared: 93.89% Adj. R square: 86.04% values are very closer.

Response Surface Methodology (RSM)

RSM gives the mathematical relationship between the output response and the independent variables are unknown [23]. T. Kim *et al.* [24-29] studied the response surface methodology by employing it in steel. The second-order model was used in the resistance spot welding process. The Box-Behnken design was adopted to formulate a useful regression model. Optimum welding conditions were determined by desirability approach. Among 17 experimental Runs, 8 Residues lie in the centre and almost all the residue lie in the trend line. Two outliers present in the normal probability.

Residual plots for TSFL

The Response surface of tensile shear fracture load was obtained for the analysis of the interaction effects. Fig. 2(a), 2(b) and 2(c) show that, when there is an increase in factor A and B, there will be an increase in 10.5 kN. Fig. 2(a), 2(b) and 2(c) also show that the peak value is attained during higher A and higher B. At lower and higher levels of A and C shows dip in the response, whereas in the middle level of A and C, Steep increase of response as noticed. It is due to Peak Value as attained in the highest level of A and middle level of C. In the middle level of B and C, Maximum Response is obtained.

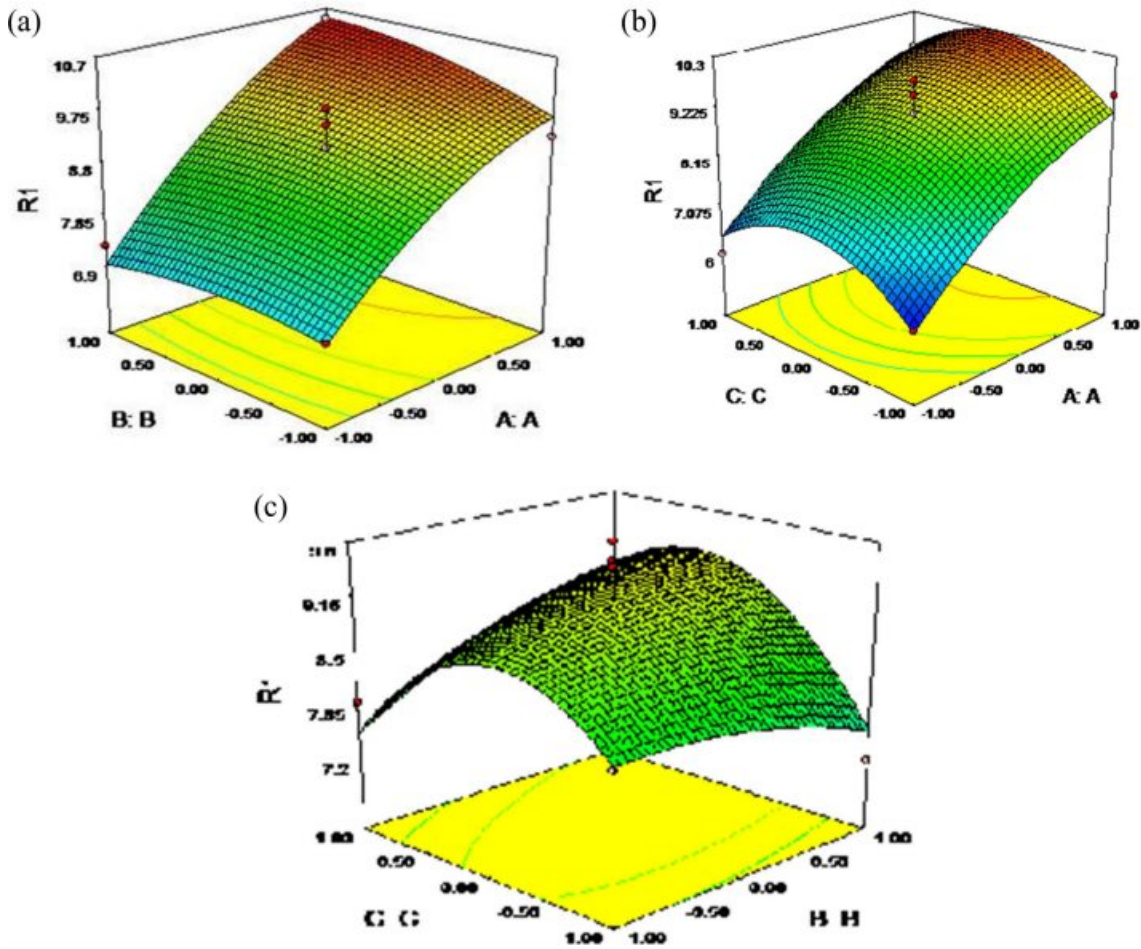


Fig. 2. Three dimensional plot for the resistance welding parameter with TSFL as response.

Response plots for Hardness

The interaction of hardness values is plotted in Fig. 3(a), (b) and (c). The similar results were obtained for the response plots for hardness. After the regression model of shear tensile strength and hardness was developed, the model adequacy examination was performed in order to substantiate the regression analysis. Fig. 3(d) shows the standard probability plot of the residual shows the proper sign and the experimental values are very closer to the straight-line pattern. It is concluded that all the data's are normally distributed and the final response equation to predict the tensile shear strength (R1) is depicted as follows in Eq. (2)

$$\begin{aligned}
 R1 \text{ (TSFL)} = & +9.18+1.54 * A+0.19 * B+0.18 \\
 & * C+0.25 * A * B+0.025 * A * C+0.47 \\
 & * B * C-0.44 * A^2-0.19 * B^2-0.96 * C^2
 \end{aligned}
 \tag{3}$$

Fig. 3(e) demonstrates the relationship between the predicted and experimental values for shear, tensile strength which indicates that both the results are very closer to the straight-line pattern.

Microstructural Studies

The interfacial zone of AISI 304 and AISI 1020 are shown in Fig. 4(a), which reveals the fabricated joints were highly inhomogeneous solidification mode. Fig. 4(b) shows the interfacial zones of fabricated resistance-welded AISI 304 and AISI1020 materials. It can be observed that the zones consist of coarse austenite and ferrite modes of solidification occurred. In addition to that presence of high chromium content in AISI 304 promoted more ferrite content. The substrate was marginally melted and re-solidified however unmixed where higher ferrite was examined as shown in Fig. 4(c). The temperature on the interface reached near to melting point attributed a formation of dendrite ferrites on the interfacial zone. These dendrite ferrites were almost normal to each weld interface as presented in Fig. 4(d) because the heat flow takes place in the same direction in each welding pass. However, when moved to weld centerline, the temperature gradient was fewer consequences equiaxed dendrites into columnar dendrites. The visual appearance of columnar dendrites at the centerline of the weld is as presented in Fig. 4(e).The flow of elements of AISI 304 in the form of grains is

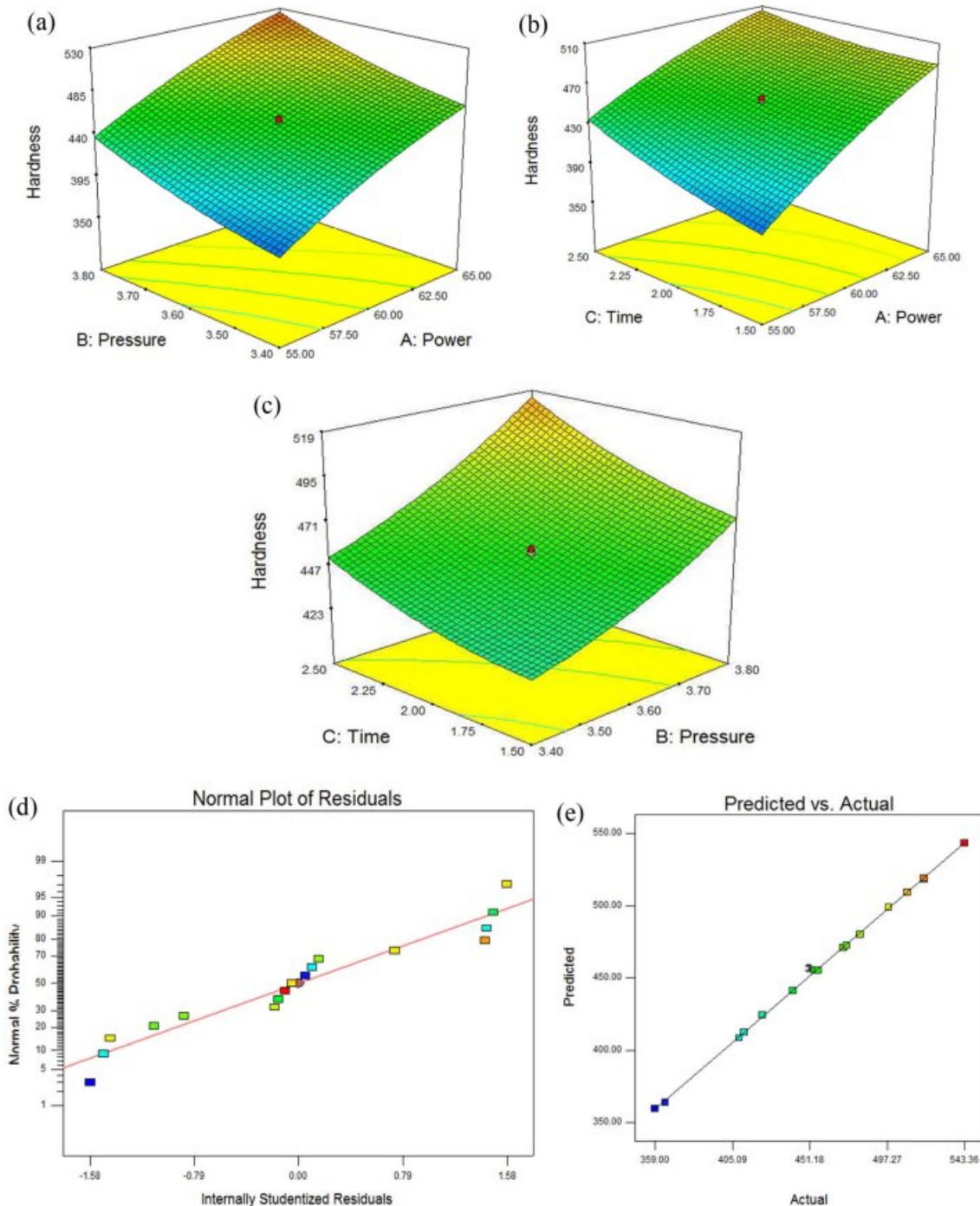


Fig. 3. (a), (b) and (c) The distinct relation among hardness on pressure, power, time. (d) and (e) Normal plot for predicted and actual values.

transferred.

EDX for AISI 304-AISI 1020 spot welded specimen

Fig. 5 shows the EDS graph which concluded that the mild steel has highest scale counts and there is no rise in counts of mild steel before 1 keV, but after the 1 keV there is a drastic change in the rise of scale counts of AISI 304 elements. Also the presence of all elements which in the form of the weight of all atoms present and net counts of all the atoms present in the specimen [30]. Amount of atoms present in the specimen

after the spot welding also listed by the application of EDX. The presence of chromium of about 13.13% and Fe content of 78.71% as shown in Table 7.

Conclusions

Based on the objective of this work RSW process was used for welding of AISI 304/AISI 1020. From the Box-Behnken analysis was carried out for ANOVA and RSM models were developed for identifying the optimal parameter to study the most influencing parameter.

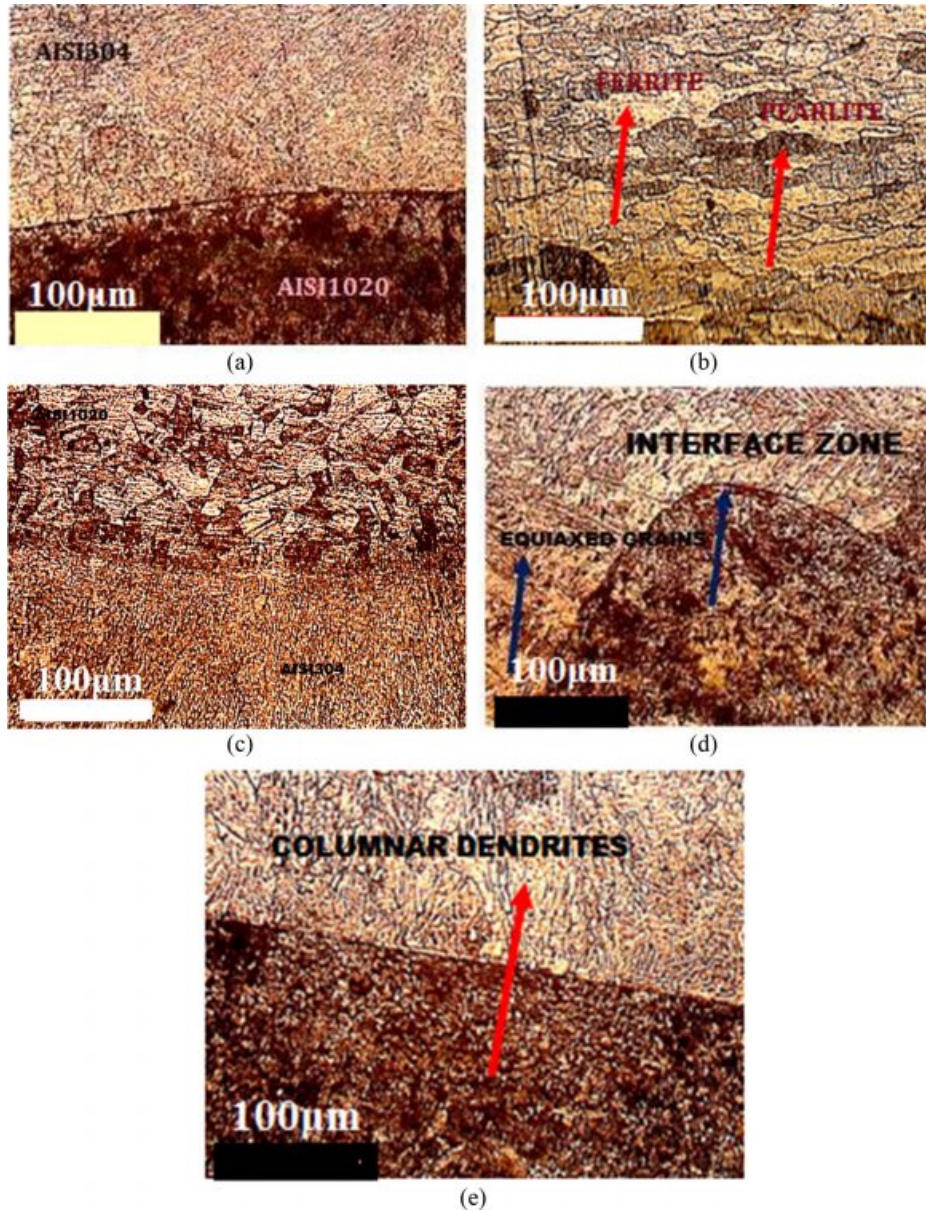


Fig. 4. Scanning Electron Microscope images of resistance spot welded joints.

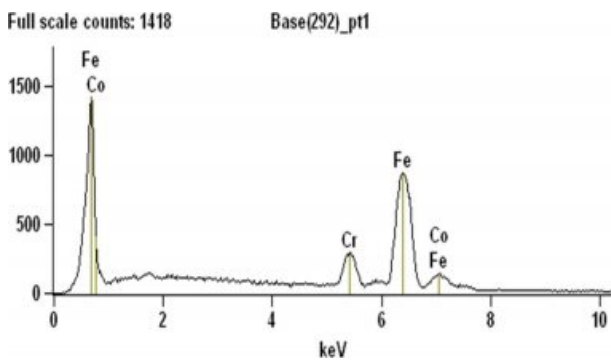


Fig. 5. EDS plot for the spot welded sample.

Table 7. Elemental Composition in Atomic weight % using EDX.

Elements	Fe	Cr	Co
Atomic weight %	78.71	13.13	8.16

The TSFL values recorded in different parameters such as pressure, time and welding current. The highest values of TSFL is 10.5 kN and the hardness of AISI 304-AISI 1020 combination is 543 VHN. The nugget diameter and Tensile strength are proportional to weld time, pressure and current. With the increase in heat input during welding, the shear - tensile strength increases within the adequate weld range due to the enlargement of nugget size.

From the RSM, it is identified that the nugget diameter

From this study, the following conclusions were drawn accordingly.

and tensile strength are influenced by weld current, followed by time and weld pressure.

The microstructural studies reveal that the welded joints are in high in homogeneous solidification mode. The weld zone consists of coarse austenite and ferrite mode, and similarly the presence of high chromium content in AISI304 promotes the formation of ferrite content.

The chemical characterisation and elemental analysis of certain samples were welded at optimum condition are executed by EDX analysis, which shows that the presence of iron, chromium and cobalt in the spot-welded joints.

References

1. H. Zhang, F. Wang, T. Xi, J. Zhao, L. Wang, and W. Gao, *Mechanical System and Signal Processing*, 62-63 (2015) 431-443.
2. P. De Tiedra, Ó. Martín, and M. López, *Corrosion. Sci.* 53 (2011) 2670-2675.
3. Jan Vinas, Lubos Kascak, and Miroslav Gres, *De Gruyter Open*. 6[1] (2016) 504-510.
4. M. Vural, A. Akkus, and B. Eryurek, *Journal of Materials Processing Technology* 176 (2006) 127-132.
5. B. Bouyousfi, T. Sahraoui, S. Guessasma, and K.T. Chaouch, *Materials and Design* 28 (2007) 414-419.
6. O. Martin, P.D. Tiedra, M. Lopez, M. San-Juan, C. Garcia, F. Martin, and Y. Blanco, *Materials and Design* 3 (2009) 68-77.
7. H.-K. Yoon, B.-H. Min, C.-S. Lee, D.-H. Kim, Y.-K. Kim, and W.-J. Park, *International Journal of Modern Physics B*. 20[25-27] (2006) 4297-4302.
8. N. Charde and R. Rajkumar, *Journal of Engineering Science and Technology*. 8 (2013) 69-76.
9. M. Ishak, L.H. Shah, I.S.R. Aisha, W. Hafizi, and M.R. Islam, *Journal of Mechanical Engineering and Sciences* 6 (2014) 793-806.
10. T.K. Mori, T. Masachika, E. Yamazaki, and Y. Watanabe, *Journal of Material Processing and Technology* 143-144 (2003) 242-248.
11. N. Kahraman, B. Gülenç, and H. Akça, *Journal of the Faculty of Engineering and Architecture of Gazi University* 17 (2002) 75-85.
12. R. Shashanka and D. Chaira, *Powder Technology* 278 (2015) 35-45.
13. H. Ma, G. Qin, P. Geng, F. Li, B. Fu, and X. Meng, *Materials & Design* 86 (2015) 587-597.
14. A. Fattah-Alhosseini and S. Vafaeian, *Egyptian Journal of Petroleum*. 24 (2015) 333-341.
15. J.H. Kim, Y. Cho, and Y.H. Jang, *Journal of Manufacturing Systems* 32[3] (2013) 505-512.
16. D. Zhao, Y. Wang, S. Sheng, and Z. Lin, *Measurement* 46[6] (2013) 1957-1963.
17. S. Aslanlar, A. Ogur, U. Ozsarac, E. Ilhan, and Z. Demir, *Materials & Design* 28 (2007) 2-7.
18. L.P. Conner, *Welding Handbook*, 8th edition, Vol. 1, P.16, American Welding Society Miami, FL, USA (1987).
19. A S M Handbook, *Welding Brazing and Soldering*, Vol.6, P.2062, ASM International, Materials Park, OH, USA (1993).
20. A.M. Pereira, J.M. Ferreira, A. Loureiro, J.D.M. Costa, and P.J. Bártolo, *Materials and Design* 31 (2010) 2454-2463.
21. M. Hessamoddin and S.F. Iradj, *Journal of Material Processing Technology* 212 (2012) 347-354.
22. Z. Hongqiang, Q. Xiaoming, B. Yang, X. Fei, Y. Haiyan, and S. Yanan, *Materials & Design* 63 (2014) 151-158.
23. G. Karthikeyan and G.R. Jinu, *Transactions of the Canadian Society for Mechanical Engineering* 40[3] (2016) 351-369.
24. K. Danial, M. Amir, and A.A. Ahmad, *Materials & Design* 61 (2014) 251-263.
25. T. Kim, H. Park, and S. Rhee, *International Journal of Production Research* 43[21] (2005) 4643-4657.
26. A. Şenaras, in "Sustainable Engineering Products and Manufacturing Technologies" (Academic Press is an imprint of Elsevier, 2019) p.187-197.
27. S.K. Beheraa, H. Meenaa, S. Chakrabortya, and B.C. Meikapab, *International Journal of Mining Science and Technology* 28 (2018) 621-629.
28. Yong Wang, Layun Deng, and Youhua Fan, *Advances in Materials Science and Engineering* 2018 (2018) 1-8.
29. Shuo Deng, Yinguang Chen, *Water Sci Technology*, 79[1] (2019) 188-197.
30. G. Karthikeyan, G.R. Jinu, and P. Vijayalakshmi, *Matéria (Rio de Janeiro)* 22[3] (2017) 1-12.